CrossMark

ORIGINAL ARTICLE

EBSA
Biophysics in Europe

The biophysics of a critical phenomenon: colonization and sedimentation of the photosynthetic bacteria *Rubrivivax gelatinosus*

Mariann Kis[1] · Gábor Sipka[1,2] · Ferhan Ayaydin[2] · Péter Maróti[1]

Abstract In response to environmental changes, the photosynthetic bacterium *Rubrivivax gelatinosus* (*Rvx.*) can switch from a planktonic lifestyle to a phototrophic biofilm. Like in critical phenomena, the colonization and sedimentation of the cells is abrupt and hard to predict causally, and the underlying biophysics of the mechanisms involved is not known. Herein, we report basic experimental observations and quantitative explanations as keys to understanding microbial turnover of aggregates. (1) The moment of sedimentation can be controlled by the height of the tube of cultivation, by the concentrations of externally added Ficoll (a highly branched polymer) and/or of internally produced polysaccharides (constituents of the biofilm). (2) The observed translational diffusion coefficient of the planktonic bacteria is the sum of diffusion coefficients coming from random Brownian and twitching movements of the bacteria and amounts to 14 $(\mu m)^2$/s. (3) This value drops hyperbolically with the association number of the cell aggregates and with the concentration of the exopolysaccharides in the biofilm. In the experiments described herein, their effects could be separated. (4) The critical conditions of colonization and sinking of the cells will be achieved if the height of the tube meets the scale height that is proportional to the ratio of the diffusion coefficient and the net mass of the bacterium. The decisive role of the web-like structure of a biofilm, the organization of bacteria from loose cooperativity to solid aggregation, and the possible importance of similar controls in other phototrophic microorganisms are discussed.

Abbreviations
Rvx. *Rubrivivax*
EPS Exopolysaccharide

Introduction

Some bacteria have two life forms during growth and proliferation. In planktonic lifestyle, they exist as single, independent cells, whereas in biofilm form, as sessile aggregates embedded within a self-produced matrix of extracellular polymeric substance (Lear and Lewis 2012; Bjarnsholt 2013) and adhere to each other and/or to a surface (Costerton and Lappin-Scott 1989; Hall-Stoodley et al. 2004; Flemming and Wingender 2010). The development of biofilms occurs in multiple stages controlled through the excretion of quorum sensing signal molecules that induce transcriptional changes in the recipient cells (Williams et al. 2007; McDougald et al. 2012). Biofilms may form on living or non-living surfaces and can be prevalent in natural, industrial, and hospital settings. Bacteria in a biofilm show much higher resistance to heavy metal ions (Kis et al. 2015, 2017) and antibiotics (Høiby et al. 2010) than planktonic bacteria due to the physical protection afforded by the extracellular matrix. As biofilms protect the bacteria, they are often more resistant to traditional antimicrobial

✉ Péter Maróti
pmaroti@sol.cc.u-szeged.hu

1 Institute of Medical Physics, University of Szeged, Rerrich Béla tér 1, Szeged 6720, Hungary

2 Biological Research Center, Hungarian Academy of Sciences, Szeged 6726, Hungary

Springer

treatments, making them a serious health risk. They can cause persistent bacterial infections like the opportunistic pathogen *Pseudomonas aeruginosa* in the lungs of cystic fibrosis patients (Hassett et al. 2010).

Photosynthetic microorganisms (diatoms, algae and cyano-, purple- and green bacteria) in terrestrial and aquatic environments can grow either as plankton or aggregates in phototrophic biofilms (mats) produced usually on surfaces when exposed to light (De Philippis et al. 2005; Roeselers et al. 2008; Nadell et al. 2009). The phototrophic biofilms have been used in widespread applications, such as wastewater treatment in constructed wetlands, bioremediation, aquaculture, and biohydrogen production ((Roeselers et al. 2007; Liao et al. 2010). The laboratory-based cultivation of phototrophic biofilms provides a valuable alternative for natural systems by allowing experimental manipulation of entire microbial systems.

Given sufficient resources for photosynthetic or respiratory growth, the biofilm will quickly grow to be macroscopic followed by a remarkable switch by the bacteria from a planktonic to a biofilm lifestyle (Steunou et al. 2013). Neither the biophysics nor the molecular and regulatory mechanisms of the transition have been elaborated to a large extent. Most progress was achieved in studies of the nonsulfur purple bacterium *Rvx. gelatinosus* by genetic analyses of its two-component regulatory system (EmbR and EmbS) and associated signal transduction cascade (Steunou et al. 2013). The inactivation of EmbRS resulted in enhanced biofilm production and fast-sinking cell aggregates in liquid. Inevitably, the operation of the regulatory system is exposed to environmental stresses which make the manifestation of the switch of lifestyles highly unpredictable.

Here we investigated aqueous cultures of *Rvx. gelatinosus* cells in test tubes where biofilm formation could easily be evoked, resulting in colonization and sedimentation of the uniformly distributed planktonic cells. The process took place collectively, suddenly, and unpredictably, like the critical phenomena of phase transitions well known in physics. A comprehensive description and interpretation of the sedimentation of bacteria are lacking in the literature. The present work focuses on the biophysical aspects and is devoted to deeper analysis and understanding of the planktonic–biofilm transition.

Materials and methods

Growing conditions

The photosynthetic purple bacterium *Rubrivivax* (*Rvx.*) *gelatinosus* were inoculated from a dense batch culture (1:100) into Sisröm's medium (Sisröm 1962) and were illuminated by tungsten lamps of 13 W•m^{-2} irradiance on the surface of the vessel (Asztalos et al. 2010). The bacteria were grown at 30 °C temperature in light and anaerobically in filled and sealed tubes. The planktonic cells were harvested at early exponential phase. Bacteria in biofilm form were harvested at late stationary phase of growth where the cells were strongly connected by their extracellular matrix. When there was a need to remove the cells from the airtight culture for external measurements, the sample was bubbled with nitrogen for 15 min to preserve the anaerobic conditions. The cell density (concentration) of the culture was estimated by counting the number of individual cells with calibrated a Bürker chamber under a light microscope.

Chemicals

Ficoll 400 (Sigma) of different concentrations (1–10 w/v%) was used to treat planktonic cells. Ficoll is a highly branched polymer formed by the copolymerization of sucrose and epichlorohydrin. It is completely non-ionic, very hydrophilic, and extremely water-soluble. Separations in Ficoll normally result in better preservation of cell function and morphology (Georgalis et al. 2012). Polygalacturonic acid (PGA) (Sigma), a major component of cell wall polysaccharides (pectins) of land plants was used here in 1 w/v% concentration.

Optical assay for sugars

As the bacterial exopolysaccharides are composed of monosaccharides including rhamnose, galacturonic acid, *N*-acetylglucosamine, and *N*-acetylfucosamine (Allen et al. 2004) and glucose at low levels, a colorimetric method for carbohydrates was applied. The soluble carbohydrate content of the biofilm was efficiently extracted by 95% ethanol in 1:1 (v: v) ratio with bacterial culture at room temperature. The yield of extraction by ethanol was significantly greater than from samples extracted with a methanol:chloroform: water solution (Chow and Landhäusser 2004). After extraction, the ethanol should be removed, as the residual ethanol can interfere with the phenol–sulfuric acid analysis. After 1 h of ethanol treatment, the sample was dried out at 40–45 °C temperature followed by rapid addition of the reagent solution of 1 ml distilled water, 1 ml 2% phenol, and 5 ml concentrated sulfuric acid (DuBois et al. 1956). After waiting 10 min for color development in the dark and cooling in a water bath at 22 °C, optical absorbance was measured by a single beam spectrophotometer (Thermo Spectronic Helios) at 488-nm wavelength. For quantitative determination of the total soluble-glucose concentration, the colorimetric method was calibrated by a series of glucose solutions of known concentrations. To avoid possible interference from other substances different

from glucose, corrections were made by running a parallel assay without phenol. The procedure was replicated five times. By assaying the same number of planktonic cells as biofilm, the sucrose content of the "biofilm + cell" system was subtracted from that of the "cells only" system to obtain the production of biofilm during the growth of the bacteria.

Time lapse video, optical-microscopy

The different phases of cell development, aggregation, and sinking of the purple bacterium *Rvx. gelatinosus* in cultivation tube were tracked by a commercial web camera. Video recording (20 fps) and images of the intact cells were captured by an Olympus IX81 inverted microscope with Cell R software (Olympus Life Science Europa GmbH, Hamburg, Germany) using a UPlanSApo 60× oil immersion objective (numerical aperture 1.35), F-View CCD camera and differential interference contrast (Nomarski) optics.

Determination of the translational diffusion constant of the bacteria

In recorded video images, arbitrary cells of *Rvx. gelatinosus* were selected for diffusion measurement. Using Image Java software, 500 individual positions of the target cell (x_i, $i = 1, ..., 500$) were marked manually during a period of 25 s. The mean displacement of the random walk of the cell ($\Sigma x_i = 0$) is expected to be zero. Absence of drift or oriented swimming (which may interfere with diffusion measurements) was checked in each occasion. The mean-square displacement ($<x_i^2>$) was calculated and found to increase linearly in time (Fig. 1). This was a clear indication of the random walk (diffusion) nature of the movement. The constant of proportionality (slope of the straight line) is $4 \cdot D$ ($6 \cdot D$) if the random movement occurs in plane (in space). The procedure was repeated with 5–10 cells and the D was obtained from the slope of the straight line fitted to the mean-square displacement ($<x_i^2>$) vs. time function. The value of D thus found did not depend on the elapsed time t.

Determination of the macroviscosity of the bacterial culture

Before sterilization and sealing of the glass tube for cultivation, a steel ball is placed in the vessel without air bubbles. As a Höppler-type viscometer, the thermostated setup can be used to determine the viscosity of the aqueous culture (η) from the time of fall (t) of the ball between to two marks on the wall of the tube and from the difference of the densities of the steel ball (ρ_{ball}) and
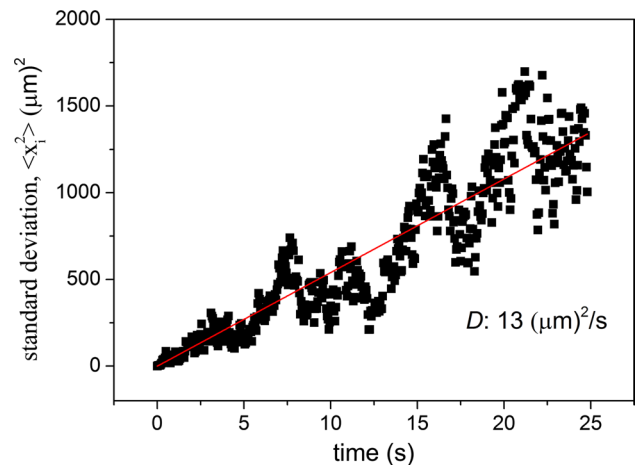

Fig. 1 Time-dependence of mean-square displacement ($<x_i^2>$) of planktonic cells *Rvx. gelatinosus* from the initial ($t = 0$) position $x_0 = 0$. The *dots* represent the average ($<x_i^2>$) for 10 walks, each having 500 steps. In the case of random (statistical or Brownian) motion of the cells in two dimensions (in *plane*), the data are expected to fit on a straight line $<x_i^2> = 4 \cdot D \cdot t$, whose slope is determined by the translational diffusion coefficient D

aqueous culture (ρ_{cult}): $\eta = K \cdot (\rho_{ball} - \rho_{cult}) \cdot t$, where K is the ball constant determined from calibration of the setup for water of known viscosity. This arrangement permitted the measurement of the viscosity of the culture in different states of the development of the photosynthetic bacteria without perturbation of the growth conditions.

Results

Growth curves of *Rvx. gelatinosus*

The inoculated cells grow photosynthetically in the illuminated anaerobic culture and undergo different phases of development (Fig. 2). After about 15 h in lag phase, the bacteria start to grow exponentially. The exponential phase terminates and turns to stationary phase with no net change of cell number after about 60 h of the inoculation under our conditions. The stationary state is followed by a slow and prolonged phase of destruction of the cells.

The purple nonsulfur bacterium *Rvx. gelatinosus* is able to produce extracellular polymeric substances that form the matrix of the biofilm, which plays a determining role in the sinking of the cells (Steunou et al. 2013). The polysaccharides start to form at the early exponential phase of cell growth. The production increases in an exponential manner and does not come to an end at the stationary phase of cell development. Due to the viscous nature of the polysaccharides, the biofilm enhances the viscosity of the culture.
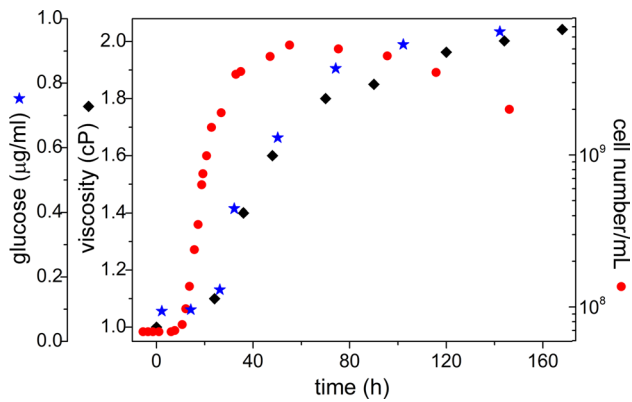
Fig. 2 Different phases of photosynthetic growth of *Rvx. gelatinosus* under anaerobic conditions. The development of glucose content (*asterisk*) and macroviscosity (*diagonal*) of the culture due to biofilm formation is delayed to that of cell concentration (*dots*). After about 60 h, the critical conditions for sudden sedimentation (sinking) are established

Sudden and collective sedimentation of bacteria

In the stationary phase of the cell growth, the uniformly distributed cells start to be clumped. The homogenous suspension becomes heterogeneous and sedimentation of coagulated particles can be observed. The configuration leading to sinking/sedimentation of the cells is established within a short period of time and its occurrence is hard to predict. The process resembles the critical phenomena well known in physics such as second-order phase transitions, fractal behavior, or ergodicity breaking. Here, we describe experimental observations of the critical phenomenon.

An important property of the collective sinking of the bacteria is its dependence on the length of the tube of cultivation (Fig. 3). Bacteria grown under otherwise identical conditions start to coagulate and sediment first in the longest tube and later in the shorter tubes. The shorter the vessel, the longer the time delay. For a quantitative evaluation, the height of the sediment was measured as a function of time, as it characterizes the beginning and the initial speed of the sedimentation (Fig. 4). Depending on the length of the tubes, the sedimentation starts at different moments and saturates after about 10 min. As not all bacteria settle at once, successive sedimentation will cause the layers to pile at the bottom of the tube.

The process can be described by a simple model. Within time t, the bacteria of constant sinking velocity v will cover a distance of $v \cdot t$ and fill up a layer of length X on the bottom of the tube. If c_0 and $A \cdot c_0$ denote the initial cell concentration in the tube and the cell concentration in the sedimented layer (A is a "factor of compression"), respectively, then the equation $(v \cdot t + X) \cdot c_0 = A \cdot c_0 \cdot X$ can be derived from the conservation of the mass of the bacteria. The height of the sedimented layer, $X(t) = v \cdot t/(1 + A)$ increases linearly with time and the maximum (saturation) value $X_{max} = h/A$ will be reached after $t_{1/2} = h/v \cdot (1-1/A)$. Although the model could have been made more realistic by using a Boltzmann distribution (see below) instead of uniform spatial distribution of the cells, even this simple treatment can rationalize the results in Figs. 3 and 4. The delay in the initiation of the sedimentation on the length of the tube can be approximated by a straight line whose slope is 30 cm/120 min ≈ 42 μm/s. This value estimates the initial velocity of decrease of the scale height (H) or of the
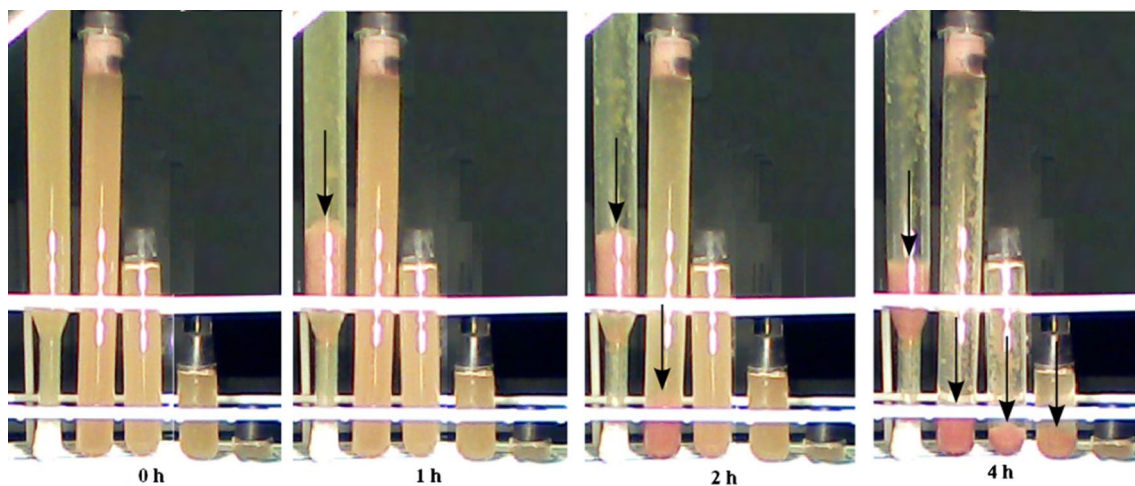

Fig. 3 Sudden sinking of *Rvx. gelatinosus* due to biofilm formation as a function of length of the culture tubes. The bacteria were grown photosynthetically to the early stationer phase (65–70 h after inoculation) and then they were distributed into tubes of different lengths (30, 15, 7, 3.5, and 1 cm from *left* to *right*). Only the *lower part* of the

longest tube (30 cm) can be seen. The sedimentation occurred spontaneously according to the lengths of the tubes; first in the longest tube (after 1 h following the transfer) and later (indicated on the pictures) in the shorter vessels
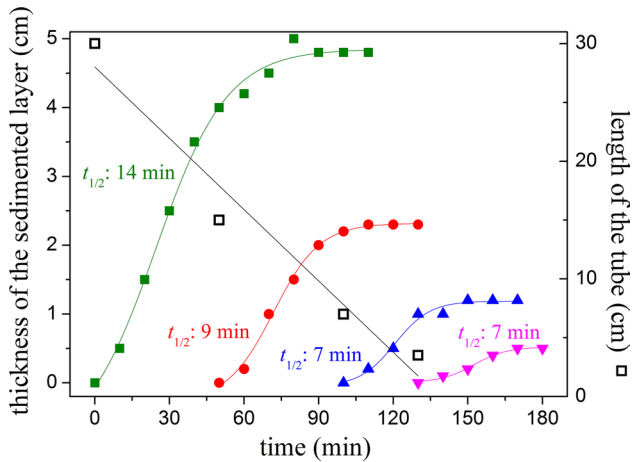
Fig. 4 Quantitative analysis of the sedimentation experiment presented on Fig. 3. The increase of the thickness of the sedimented loose layer as a function of time in tubes of four different lengths 30 cm (*green*); 15 cm (*red*); 7 cm (*blue*), and 3.5 cm (*magenta*). The ratio of tube length and thickness of the sedimented layer is constant (~6). The half times of sedimentation are indicated

diffusion coefficient (*D*) leading to the collective sinking of the bacteria (see "Discussion").

## Effect of artificial extracellular polysaccharides

The sudden and collective sedimentation of the cells was induced by extracellular polysaccharides: Ficoll 400 and polygalacturonic acid (PGA) (Fig. 5). The higher the concentrations of the Ficoll and the cell suspension, the earlier will the critical phenomenon take place. At 1% (w/v) PGA and 5% Ficoll (3×10^8 and 5×10^8 bacteria/mL cell concentrations, respectively) gradual aggregation formation and sedimentation could easily be followed by visual inspection, as shown in Fig. 5. The observed similar

behavior of extracellular polysaccharides and biofilm supports the assumption of a common cause of collective sinking. The Ficoll (and particularly the PGA) may have structural and functional analogy to the extracellular polysaccharides produced by the bacteria. The cells of *Rvx. gelatinosus* are not only able to produce the polymers but also to catch the polymer chains produced by the neighbors. This makes the bacterial system able to form web-like structures with all of the known consequences including the switch from planktonic to biofilm lifestyles. Similar phenomena are not observed with other purple photosynthetic bacteria even if a branch-forming agent is present. The PGA and Ficoll proved to be ineffective in triggering coagulation and sinking of *Rba. sphaeroides* cells (see the leftmost tube of Fig. 5).

It is interesting to follow the temporal and spatial change in cell concentration in the test tube during the sedimentation process. Figure 6 represents the spatial distribution of the bacteria along the 14-cm-long tube at selected times after addition of 5% Ficoll. While the mean value of the distribution (point of mass of the bacteria) shifts downwards progressively, the integral of the curves (total mass of the bacteria) remains constant.

A different aspect of the Ficoll treatment of the bacterial culture can be appreciated by measurement of the translational diffusion coefficient (*D*) of the individual cells in planktonic lifestyle where the effect of biofilm formation is negligible (Fig. 7). The measurement was carried out after the addition of Ficoll to the culture but long before the appearance of signs of collective sinking. A significant reduction in *D* of intact cells of *Rvx. gelatinosus* can be seen with an increase in the concentration of Ficoll. Qualitatively, the cells become more and more connected at higher and higher Ficoll concentrations with consequent decrease in the mobility of the individual cells. The decrease in *D* can be attributed to the increase of the (macro)viscosity

Fig. 5 Sedimentation of bacteria *Rvx. gelatinosus* induced by 5% Ficoll 400 and 1% polygalacturonic acid (PGA) in cultures of different cell concentrations. For comparison, the leftmost tube contains *Rba. sphaeroides* of 5×10^8 cell/mL concentration, which does not sediment upon addition of 5% Ficoll. After 1 h, the aggregation and subsequent sedimentation begin in the tube of largest cell concentration and in the tube of PGA
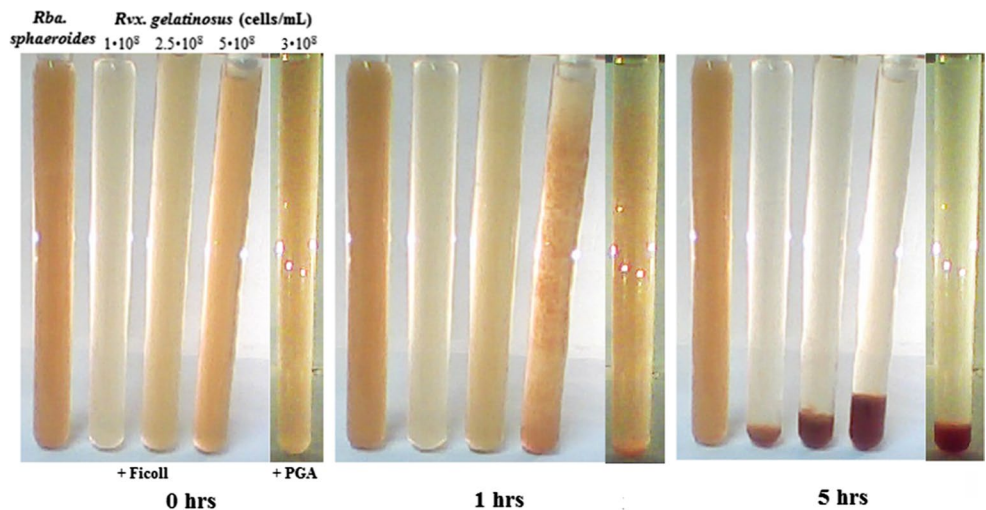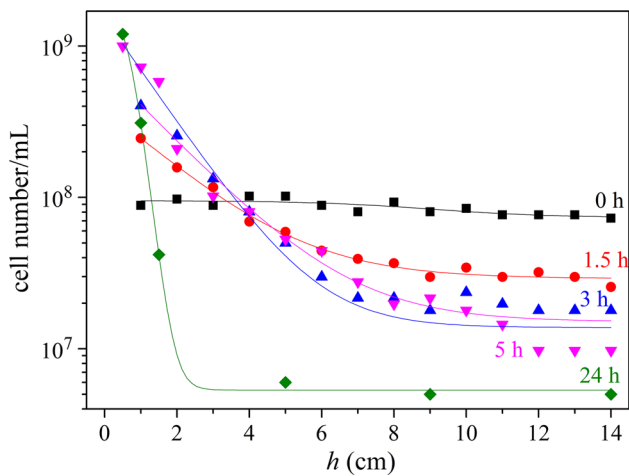
Fig. 6 Spatial distribution of cells *Rvx. gelatinosus* along a $h = 14$-cm-long test tube at different time points (0, 1.5, 3, 5, and 24 h) after start of colonization and sedimentation by 5% Ficoll. The initial cell concentration of uniformly distributed bacteria was 1×10^8 cells/mL. The cell concentrations at different heights (*points on the graph*) were determined by measurement of the optical absorption followed by calibration using known aliquots of the bacterial culture. The curves are the best fits of the Boltzmann distribution (Eq. 1) to the points with scale heights H of the major (87%) component ∞ (0 h), 5.3 cm (1.5 h), 2 cm (3 h), 1 cm (5 h), and 0.4 cm (24 h)
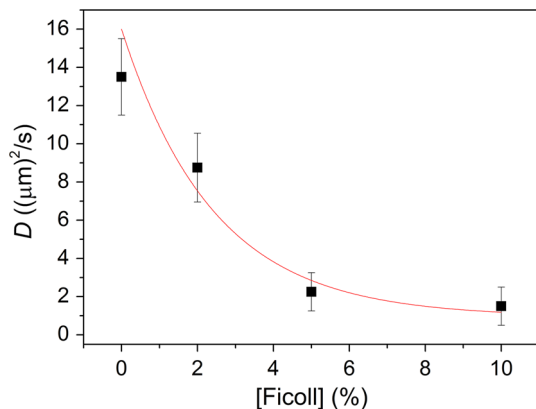

Fig. 7 Decrease of the translational diffusion coefficient of intact planktonic cells of *Rvx. gelatinosus* as a function of Ficoll concentration (expressed in w/v%) of the culture at room temperature (25 °C). The cell concentration is 1×10^8 bacteria/mL. The curve is the least square best fit of Eq. (8) to the data points

of the solution and to the increase in the Stokes (hydrodynamic) radii of the cells. The former is not essential. While 10% Ficoll causes about one order of magnitude drop of the diffusion coefficient, the (macro)viscosity of the 10% Ficoll solution ($\eta \approx 2$ cP) is only about twice as large as that without Ficoll ($\eta \approx 1$ cP) in good analogy with that of biofilm (see Fig. 2). The branched polymer Ficoll produces similar web-like structures in planktonic cell culture as cells experience in a biofilm and causes significant increase in the

Stokes radius of the bacterium. One can thus argue that not the (somewhat) increased viscosity of the culture but the connectivity among the cells is responsible for the decrease in mobility.

Diffusion coefficients in biofilm

The mobility of the bacteria depends on its lifestyle: while cells in planktonic form are monomeric and highly independent, in biofilm they tend to colonize into aggregates (Fig. 8). Both the association and the increased exopolysaccharide (EPS) content of the solution will decrease the mobility of the cells (Fig. 9). As these factors usually appear together (biofilm formation), the separation of their overlapping effects is challenging. If we selected different bacterium associates with about the same association number (N) in the view field of the microscope, and tracked
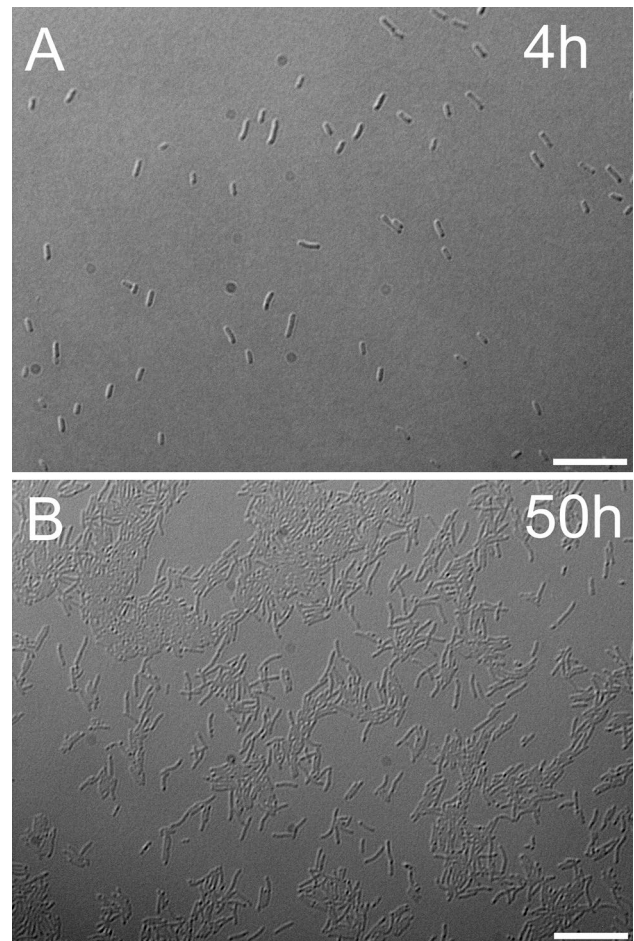

Fig. 8 Microscopy images of *Rvx. gelatinosus* cells in the exponential (4 h) and stationary phase (50 h) of growth. During exponential growth, 2–4-μm-long planktonic cells are exclusively in single celled form (**a**), cells of stationary phase, however, tend to colonize and form doublets, triplets, and higher orders of aggregates (**b**). *Scale bars* are 10 μm

EPS glucose (μg/mL) (*10)●
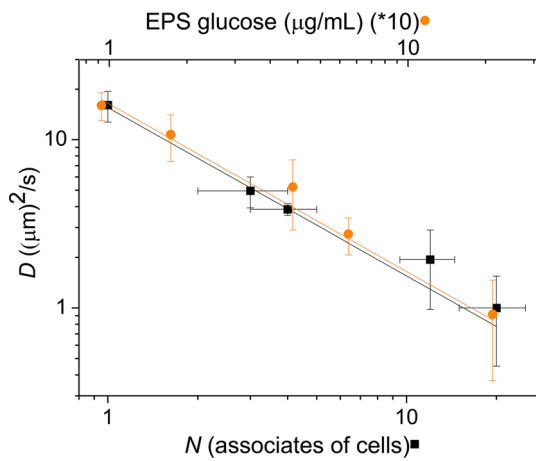
D (μm)^2/s)

N (associates of cells)■

Fig. 9 Translational diffusion coefficient (*D*) of cells *Rvx. gelatinosus* as a function of number of aggregates (*N*) and amount of exopolysaccharide (*EPS*) produced by the cells during growth. The *standard errors* of the means are indicated

their pathways, then the sole effect of aggregation on the diffusion coefficients (*D*) would be obtained (the EPS content remained constant). The aggregation will affect the measured diffusion coefficient due to increased Stokes radius the higher the degree of association is, the smaller is the diffusion coefficient. On the other hand, if only monomeric bacteria were marked in different samples taken from the culture for evaluation, and the corresponding EPS content was determined, then the sole effect of biofilm formation on the diffusion coefficient would be granted because the degree of association would not change (it would remain monomeric). We see that the produced biofilm affects the measured diffusion coefficient due to the increased viscosity of the culture: the higher the EPS content is, the smaller is the measured diffusion coefficient. Because of the statistical nature of the determination of all quantities (EPS content, *N* and *D*), the standard errors of the means are necessarily large. In double logarithm representations, the corresponding data sit on straight lines that cross the error ellipsis of the mean values.

Discussion

During the late phases of growth of the photosynthetic bacterium *Rvx. gelatinosus*, sudden colonization and sedimentation of the cells occurs. While the basics of the molecular mechanism, the regulatory pathways, and the physiological impact (switch of the lifestyle from planktonic to biofilm) have been largely revealed (Steunou et al. 2013), the biophysics of the process remained completely obscure. In the present study, we have attempted to address this issue. Critical phenomena are described using the highly advanced

methods of statistical physics (Nishimori and Ortiz 2010) but here an elementary and descriptive analysis based on causal relations of physics will be presented.

Distribution of bacteria in vertical tubes

A thin test tube of length *h* in a horizontal position is uniformly filled with cell culture of concentration c_0. After a lengthy period in a vertical position, a sedimentation equilibrium in the gravitational field will be established with a vertical profile of cell density *c*(*x*) described by the Boltzmann relation:

$$c(x) = c_0 \cdot \frac{h}{H} \cdot \frac{\exp\left(-\frac{x}{H}\right)}{1 - \exp\left(-\frac{h}{H}\right)}. \tag{1}$$

Here, *x* denotes the height from the bottom of the vertical tube and *H* is defined as the scale height:

$$H = \frac{k_B T}{m_{net} g}. \tag{2}$$

The buoyant correction of the mass of the cell reduces *m* to $m_{net} = m \cdot (1 - \rho_w / \rho_{bac})$, where ρ_w and ρ_{bac} are the mass density of water and bacterium, respectively, *g* is the gravitational acceleration, and $k_B T$ is the Boltzmann term. The scale height *H* is inversely proportional to the net mass of the bacterium: the larger the m_{net} is, the smaller is *H*. The pre-exponential factor in Eq. (1) is calculated from the conservation of the bacterial mass in both positions of the test tube. The set of sedimentation distributions of the cells induced by Ficoll could be well approximated by the Boltzmann equation with progressively decreasing scale heights as the duration of the treatment increases (Fig. 6).

The Boltzmann distribution shows that, for settling to occur, the gravitational potential energy $m_{net} \cdot gh$ between the top and bottom must be bigger than the thermal energy. In other words, the cells float when *h* ≤ *H* but start to settle down when *h* > *H*. By changing the scale height *H* to the length of the tube *h*, transition from uneven (Boltzmann-) distribution [partial (*h* > *H*) or complete (*h* ≫ *H*) sedimentation] to uniform distribution (*h* ≤ *H*) will be obtained. Due to the exponential function in Eq. (1), the sinking or floating is highly sensitive to a ratio of *h*/*H* around 1. Similar abrupt changes are observed in the critical phenomena of statistical physics like phase transitions (Domb and Lebowitz 2001).

The simple conclusion from the Boltzmann distribution is manifested in experiments where the sedimentation is induced by an increase of the length of the tube (Fig. 3) or by the addition of Ficoll (Fig. 5). If the length of the tube exceeds the scale height (*h* > *H*), then indeed,

colonization and sinking of the bacteria will occur. In contrast, the distribution of the cells remains uniform and no sedimentation can be observed in shorter tubes ($h < H$). In a parallel experiment, the length of the tube was kept constant and the scale height was modified by the branched polymer Ficoll at different concentrations. Here again, the simple principle operates: the Ficoll (mainly through colonization) will increase the net mass of the bacterium and therefore decrease the scale height (see Eq. 2). As soon as H becomes as small as h, sedimentation will take place.

Further experiments are required to identify the factors and mechanisms that contribute to modification of the scale height that leads to either suspension or sedimentation of the bacterium *Rvx. gelatinosus*. We anticipate that the active motion of the bacteria should play a decisive role.

Random and slow motion of *Rvx. gelatinosus* in planktonic lifestyle

The bacteria showed slightly curved and rod-shaped morphology (Fig. 8), as well as Gram-negative staining and motility in accordance with literature data (Imhoff and Trüper 1989). In the absence of long polar flagella, however, the bacteria possess very slow motility thanks to the small thin filamentous hair-like appendages (pili and fimbriae) on the cell surface. Similar (twitching) motility on moist solid surfaces is routinely observed in other microorganisms like *Pseudomonas aeruginosa* (Henrichsen 1983). Therefore, the observed motion of the planktonic cell is composed of passive (Brownian) and active (twitching) random movements. It can be shown (Appendix 1) that the superposition of two independent random walks of diffusion coefficients D_1 and D_2 results in also a random motion whose diffusion coefficient D is the sum of those of the components: $D = D_1 + D_2$. Applying to the composed motion of the active bacteria:

$$D = D_{Brown} + D_{twitch}. \tag{3}$$

To characterize the biologically active form of movement, the Brownian diffusion should be separated from the random movement of twitching. This can be done by fixing the bacteria *Rvx. gelatinosus* in 10% formaldehyde. The treatment kills the physiological activity and thus the self-movement of the cell without significant distortion of the hydrodynamics. The diffusion coefficient of the immobilized bacteria can be estimated from the small rate of the sedimentation or directly from the Einstein–Smoluchowski relation of diffusion:

$$k_B T = D \cdot 6\pi \eta R_s, \tag{4}$$

with reasonable choice of the hydrodynamic parameters of the cell (macroviscosity $\eta \approx 1 \times 10^{-3}$ kg·s^2 and stokes radius $R_s \approx 2$ μm). The procedures render a limiting

(Brownian) diffusion coefficient of $D_{Brown} \approx 0.1$ (μm)^2/s, that is significantly (more than one order of magnitude) smaller than the measured diffusion coefficient D of intact cells (see Figs. 7, 9). This means that primarily the active movement of the bacteria are responsible for the observed larger displacement.

Active random motion of *Rvx. gelatinosus* prohibits the cells from sinking

The calculated value of the scale height is usually much less than the heights of tubes (water columns). The difference of the mass densities is $(\rho_{bac}-\rho_w) \approx 80$ kg/m^3 for most of microorganisms but can be as small as 10 kg/m^3 for phototropic cells (Overmann et al. 1991). The replacement of these values and the approximate 1-μm linear size of the bacterium into Eq. (2) will give $H = 5$ and 40 μm scale heights, which are much below the possible tube heights ($H \ll h$). Therefore, the bacteria without active motion sink to the bottom of the tubes. After agitation, the bacterial culture kept for a longer period of time (for weeks) in the dark in a refrigerator performs slow sedimentation. The active random motion of the bacterium should result in the increase of H above h and this condition assures the even distribution (buoyancy) of the bacteria in the tube of culture.

Replacing Eqs. (3) and (4) into Eq. (2), a more general form of the scale height can be obtained, which contains both the passive Brownian and the active (twitching) random motions:

$$H = \frac{k_B T}{m_{net} g}\left(1 + \frac{D_{twitch}}{D_{Brown}}\right). \tag{5}$$

It is worthwhile to analyze the thermal equilibrium. In the absence of the active movement of the bacterium, the cell carries out a Brownian walk only and is in thermal equilibrium with the culture. If, however, the bacterium has additional (active) movement, then the temperature of the ensemble of the cells will be by a factor of D_{twitch}/D_{Brown} higher than the temperature T of the bulk (aqueous culture). The energy flow driven by the temperature difference is compensated always by the free energy production accompanied by the active motion. Therefore the temperature difference is conserved as long as the bacterium remains active. If, however, the active motion terminates, then the temperatures will be equilibrated between the bulk and the cells. In this case, the increase of the temperature of the bulk will be not significant because the number of the cells (and thus their heat capacity) is negligible to the number (to the heat capacity) of water molecules in the culture.

Based on Eq. (5), two factors can be made responsible for changes of H (1) diffusion coefficient D_{twitch} derived

from the active motion of the bacterium and (2) the net mass m_{net} of the bacterium. Whereas the active motion increases, the net mass decreases the scale height and thus the probability to get even distribution of the cells in the tube. Both quantities may change during growth of the bacteria (Fig. 2). In the lag phase or in the early exponential phase, the cells are in low concentrations, do not aggregate (the m_{net} is small), and move independently (planktonic lifestyle) with high diffusion coefficient (D_{twitch} is high compared to D_{Brown}). In late exponential and stationer phases, however, a web of EPS is formed, the cells tend to associate, and the aggregates act as single particles with increased m_{net}. Simultaneously, the movement of the cells (or aggregates) will be slowed down due to the network whose tendency can be formally expressed as decrease of the D_{twitch}/D_{Brown} ratio. The two effects are unidirectional and favor the sedimentation by decrease of H. We managed to introduce experimental techniques for possible separation of the two effects and to study the critical conditions around $H/h = 1$, which serves as a gate leading to collective and sudden sinking/sedimentation of the cells.

Separation of decrease of diffusion and increase of net mass of the cells

1. The decrease of the diffusion was studied under two different conditions where one of the two variables was held constant
    1.1. Planktonic cells treated by Ficoll. As in a planktonic lifestyle the cells do not associate, the sole effect of Ficoll was manifested in decrease of the diffusion coefficient (Fig. 7). A simplified binding model of multiple and independent binding sites can account for the decrease of the observed diffusion constant.

If $[P]$ and $[B]$ denote the concentrations of the polysaccharide (polymer) and bacterium, respectively, and P has n binding sites with all identical K binding constant for B, then

constants D_{free} and D_{bound} weighted by the corresponding concentrations:

$$D = \frac{D_{free} \cdot [B_{free}] + D_{bound} \cdot [B_{bound}]}{[B_{free}] + [B_{bound}]}. \tag{7}$$

By use of $[B_{tot}] = [B_{free}] + [B_{bound}]$, we get

$$D = D_{bound} + (D_{free} - D_{bound}) \cdot \frac{[B_{free}]}{[B_{tot}]}. \tag{8}$$

The concentration and the binding constant should be measured in number/volume and volume/number, respectively. The range of cell concentration used here is $[B_{tot}] = 10^9–10^{12}$ cells/L, and that of Ficoll should be calculated from the molecular mass (4×10^5 g/mol) 10% (w/v) Ficoll corresponds to $[P] = 0.1$ g/mL $= 0.25$ mM $= 1.5 \times 10^{20}$ molecules/L. In our experiment represented by Fig. 7, $[B_{tot}]$ was 1×10^{11} cells/L and the concentration of Ficoll increased from 0 to 10%. The values predicted by the model satisfactorily fit the observed data. The choice of $n = 1$ has proved to be a reasonable value because of the sizes of the partners: the Stokes radii of the bacterium and the polymer are 2 μm and 10 nm, respectively. The binding constant amounts $K = 10^{-19.3}$ L/number of molecules and the limiting diffusion coefficients are $D_{free} = 16.5$ (μm)^2/s and $D_{bound} \cong 0$. We discussed above that the diffusion constant of the Brownian movement of the cell is very small (≈ 0.1 (μm)^2/s). Additionally, the cell is bound to the polymer, which decreases further the diffusion constant of the bound bacterium.

1.2. Bacteria in biofilm life style. The amount of biofilm (the produced EPS) was measured in different states of the development, and only the monomeric cells were selected for diffusion measurement (Fig. 9). Towards the late log/stationary phase of the culture, the biofilm production increased steadily while the diffusion coefficient of the monomeric cells decreased progressively. In double logarithm representation, a straight line of

$$\frac{[B_{free}]}{[B_{tot}]} = \frac{1 - n \cdot \frac{[P]}{[B_{tot}]} - \frac{1}{K \cdot [B_{tot}]} + \sqrt{\left(1 - n \cdot \frac{[P]}{[B_{tot}]} - \frac{1}{K \cdot [B_{tot}]}\right)^2 + \frac{4}{K \cdot [B_{tot}]}}}{2}. \tag{6}$$

The total amount of bacteria and the amount of cells not bound to P are denoted by lower cases "tot" and "free", respectively. Whereas the random walk of the free (planktonic) bacteria is characterized by the maximum diffusion constant D_{free}, the bound bacteria have much reduced mobility with small diffusion constant D_{bound}. The observed diffusion constant is the average of the limiting diffusion

slope −1 was obtained that reflected inverse proportionality between the amount of biofilm in the culture and the diffusion coefficient of the monomeric cells. This is quite a reasonable result: in the absence of other changes, the diffusion coefficient should be in inverse relationship with the microviscosity of the culture modified by the biofilm (see Eq. 4).

2. Increase in the net mass of the cells. While the amount of biofilm (EPS) was kept constant, cell aggregates of different association numbers (N) were selected. Due to the adjusted experimental conditions, the sizes of the aggregates changed only and not the microviscosity of the suspension as the biofilm concentration remained unchanged. Therefore, the observed changes in diffusion could be attributed solely to the aggregation of the cells. We found that the diffusion coefficients decreased sharply upon increase of N (Fig. 9). In double logarithm scale, the plot could be approximated by a straight line of slope –1, which indicated inverse proportionality between the diffusion coefficient and the aggregation number over wide ranges of the variables. This observation can be supported by the conclusion of a simple model based on a one-dimensional random walk (Appendix 2) the diffusion coefficient of an N-meric aggregate is inversely proportional to the association number.

The critical phenomenon of collective sinking of bacteria *Rvx. gelatinosus* comes to pass when the decrease of the scale height meets the tube length. The drop of H is evoked both by the increase of the net mass of the bacteria and by the increase of microviscosity of the culture due to biofilm formation. According to Eq. (5), their effects interfere and initiate the sudden change of lifestyle of the bacteria from planktonic to biofilm which is advantageous in the case of stresses such as limited light or nutrients (Jarrell and McBride 2008; Yildiz and Visick 2009).

Appendix 1

The overlap of two independent random movements results in random movement

Thesis If two particles are undergoing two independent random motions simultaneously, then the observed (resultant) motion is also random motion. If the diffusion coefficients of the components are D_1 and D_2, then the diffusion coefficient of the resultant motion is the sum of those of the components: $D = D_1 + D_2$.

Proof The probability density function of a particle carrying out one-dimensional random movement along a straight line (x-axis) starting from point $x = 0$ can be described by a Gaussian function of standard deviation of the mean σ:

$$f(x) = \frac{1}{\sqrt{2\pi \cdot \sigma}} \exp\left(-\frac{x^2}{2 \cdot \sigma^2}\right). \tag{9}$$

The function offers the probability of finding the particle in interval dx around x. The density function is normalized to unity: $\int_{-\infty}^{+\infty} f(x)dx = 1$, as the particle can be in any case found somewhere on the x-axis. If the particle accomplishes two random motions of σ_1 and σ_2 standard deviations simultaneously and independently, then density function of the resultant movement $F(x)$ is given by the convolution of the density functions of the component movement $f_1(x)$ and $f_2(x)$:

$$F(x) = \int_{-\infty}^{+\infty} f_1(x') \cdot f_2(x - x')dx'. \tag{10}$$

If the particle gets to an arbitrary position x' due to the first type of random movement, then the second type of random motion has to bring the particle to the final position x. The coordinate x' scans the whole axis. This is the meaning of the convolution in Eq. (10).

After insertion of the corresponding Gaussian functions of Eq. (9) for f_1 and f_2, and calculation of the integration, we will get a normalized Gaussian function for the density function of the resultant motion:

$$F(x) = \frac{1}{\sqrt{2\pi \cdot \left(\sigma_1^2 + \sigma_2^2\right)}} \exp\left[-\frac{x^2}{2 \cdot (\sigma_1^2 + \sigma_2^2)}\right]. \tag{11}$$

This means that the resultant motion is also random motion whose variance (square of the standard deviation) is the sum of the variances of the components:

$$\sigma^2 = \sigma_1^2 + \sigma_2^2. \tag{12}$$

Because the variance is proportional to the diffusion coefficient ($\sigma^2 = 2D\cdot t$ in straight line (one dimension), $\sigma^2 = 4D\cdot t$ in plane (two dimensions) and $\sigma^2 = 6D\cdot t$ in space (three dimensions), where t is the time of random walk), the diffusion coefficients add up independently on the dimension of the space where the diffusion takes place:

$$D = D_1 + D_2. \tag{13}$$

Appendix 2

Diffusion coefficient of *N*-meric aggregate

Consider the particle executing one-dimensional random walk of step size a. It steps either to the left or to the right with probability $p = \frac{1}{2}$. Assume that N particles form an associate (N-meric aggregate). If k members of the associate step to the right and the remaining ($N–k$) members to

the left, then the displacement of the N-meric aggregate will be $\frac{2k-N}{N} \cdot a$ occurring with probability of $P_k = \binom{N}{k} \cdot p^k \cdot (1-p)^{N-k}$. This is a binominal distribution with zero mean value and we get $\sigma^2 = \left(1 - \frac{N-1}{N} \cdot 4p\,(1-p)\right) \cdot a^2$ for the standard deviation of the mean after elementary calculations. As the diffusion coefficient D is proportional to σ^2 and $p = \frac{1}{2}$, the diffusion coefficient of the N-meric aggregate is N times smaller than D_0, the diffusion coefficient of the monomer:

$$D = \frac{D_0}{N}. \tag{14}$$

References

Allen MS, Welch KT, Prebyl BS, Baker DC, Meyers AJ, Sayler GS (2004) Analysis and glycosyl composition of the exopolysaccharide isolated from the floc-forming wastewater bacterium *Thauera* sp. MZ1T. Environ Microbiol 6(8):780–790

Asztalos E, Italiano F, Milano F, Maróti P, Trotta M (2010) Early detection of mercury contamination by fluorescence induction of photosynthetic bacteria. Photochem Photobiol Sci 9:1218–1223

Bjarnsholt T (2013) The role of bacterial biofilms in chronic infections. APMIS Suppl 136:1–51

Chow PS, Landhäusser SM (2004) A method for routine measurements of total sugar and starch content in woody plant tissues. Tree Physiol 24:1129–1136

Costerton JW, Lappin-Scott HM (1989) Behavior of bacteria in biofilms. Am Soc Microbiol News 55:650–654

De Philippis R, Faraloni C, Sili C, Vincenzini M (2005) Populations of exopolysaccharide-producing cyanobacteria and diatoms in the mucilaginous benthic aggregates of the Tyrrhenian Sea (Tuscan Archipelago). Sci Total Environ 353:360–368

Domb C, Lebowitz JL (2001) Phase transitions and critical phenomena, vol 19. Academic Press, San Diego

DuBois M, Gilles KA, Hamilton JK, Rebers PA, Smith F (1956) Colorimetric method for determination of sugars and related substances. Anal Chem 28(3):350–356

Flemming HC, Wingender J (2010) The biofilm matrix. Nat Rev Microbiol 8:623–633

Georgalis Y, Philipp M, Aleksandrova R, Krüger JK (2012) Light scattering studies on Ficoll PM70 solutions reveal two distinct diffusive modes. J Colloid Interface Sci 386(1):141–147

Hall-Stoodley L, Costerton JW, Stoodley P (2004) Bacterial biofilms: from the natural environment to infectious diseases. Nat Rev Microbiol 2:95–108

Hassett DJ, Korfhagen TR, Irvin RT, Schurr MJ, Sauer K, Lau GW, Sutton MD, Yu H, Hoiby N (2010) *Pseudomonas aeruginosa* biofilm infections in cystic fibrosis insights into pathogenic processes and treatment strategies. Expert Opin Ther Targets 14:117–130

Henrichsen J (1983) Twitching motility. Annu Rev Microbiol 37:81–93

Høiby N, Bjarnsholt T, Givskov M, Molin S, Ciofu O (2010) Antibiotic resistance of bacterial biofilms. Int J Antimicrob Agents 35(4):322–332

Imhoff JP, Trüper HG (1989) Purple nonsulfur bacteria. In: Bergey DH, Krieg NR, Holt JG (eds) Bergey's manual of systematic bacteriology. Williams and Wilkins, Baltimore, pp 1635–1709

Jarrell KF, McBride MJ (2008) The surprisingly diverse ways that prokaryotes move. Nat Rev Microbiol 6:466–476

Kis M, Sipka G, Asztalos E, Zs Rázga, Maróti P (2015) Purple nonsulfur photosynthetic bacteria monitor environmental stresses. J Photochem Photobiol B Biol 151:110–117

Kis M, Sipka G, Maróti P (2017) Stoichiometry and kinetics of mercury uptake by photosynthetic bacteria. Photosynth Res 132(2):197–209

Lear G, Lewis GD (eds) (2012) Microbial biofilms: current research and applications. Caister Academic Press, Norfolk, UK. ISBN 978-1-904455-96-7

Liao Q, Wang Y-J, Wang Y-Z, Zhu X, Tian X, Li J (2010) Formation and hydrogen production of photosynthetic bacterial biofilm under various illumination conditions. Biores Technol 101:5315–5324

McDougald D, Rice SA, Barraud N, Steinberg PD, Kjelleberg S (2012) Should we stay or should we go: mechanisms and ecological consequences of biofilm dispersal. Nat Rev Micro 10:39–50

Nadell CD, Xavier JB, Foster KR (2009) The sociobiology of biofilms. FEMS Microbiol Rev 33(1):206–224

Nishimori H, Ortiz G (2010) Elements of phase transitions and critical phenomena. Oxford University Press, Oxford

Overmann J, Lehmann S, Pfennig N (1991) Gas vesicle formation and buoyancy regulation in *Pelodictyon phaeoclathratiforme* (Green sulfur bacteria). Arch Microbiol 157:29–37

Roeselers G, Norris TB, Castenholz RW, Rysgaard S, Glud RN, Kühl M, Muyzer G (2007) Diversity of phototrophic bacteria in microbial mats from Arctic hot springs (Greenland). Environ Microbiol 9(1):26–38

Roeselers G, Loosdrecht MC, Muyzer G (2008) Phototrophic biofilms and their potential applications. J Appl Phycol 20:227–235

Steunou AS, Liotenberg S, Soler M-N, Briandet R, Barbe V, Astier Ch, Ouchane S (2013) EmbRS a new two-component system that inhibits biofilm formation and saves *Rubrivivax gelatinosus* from sinking. Microbiol Open 2(3):431–446

Williams P, Winzer K, Chan WC, Camara M (2007) Look who's talking: communication and quorum sensing in the bacterial world. Philos Trans R Soc Lond B Biol Sci 362:1119–1134

Yildiz FH, Visick KL (2009) Vibrio biofilms: so much the same yet so different. Trends Microbiol 17:109–118